ORIGINAL PAPER

Effect of Nanosilica and Nanoclay on the Mechanical, Physical, and Morphological Properties of Recycled Linear Low Density Polyethylene/Rice Husk Composites

Wagih Abdel Alim Sadik[1] · Abdel Ghaffar Maghraby El Demerdash[1] · Rafik Abbas[1] · Alaa Bedir[1]

Abstract

The principal objective of this study was to assess the capability of waste rice husk fibers as reinforcement for recycled plastics. The fabrication of Wood-plastic composites (WPCs) based on rice husk (RH) fibers and recycled linear low polyethylene in the presence of maleic anhydride grafted polyethylene (3 phc) were made by melt blending method. The impact of nanosilica and nanocaly, at different concentrations (2, 4, and 6 phc) on morphological, physical–mechanical and thermal properties of the prepared WPCs were studied to distinguish the most efficient nanoparticle. The highest improvement of mechanical properties was achieved at 6phc nanosilica loading and 4phc nanoclay. At a high level of nanoclay loading (6phc), increased population of clay pellets leads to agglomeration, and stress transfer gets blocked. Izod impact strength was decreased by the incorporation of different nanoparticles in contrast with the hardness. The addition of different nanoparticles decreased the water absorption and thickness swelling of composites. The interaction of the rice husk fibers with the polymer matrix as well as the impact of nanosilica and nanoclay in the improvement of the adhesion was shown by scanning electron microscopy (SEM). In addition, the thermal stability showed slightly improved by the addition of nanoparticles, but there are no perceptible changes in the values of melting temperature by increasing the nanosilica and nanoclay content. The degree of crystallinity (X_c) of the composites decreased with the incorporation of RH fibers and increased with the addition of nanoparticles. The finding demonstrated that WPCs treated by nanosilica had the most elevated properties than nanoclay.

Keywords Recycled plastic · Rice husk · Nanosilica · Nanoclay · Wood-plastic composites

Introduction

In recent times, nanoparticles and natural fibers have been increasing consideration in the fabrication of composite because of two causes. The first is to promote the properties of the composites by including nanoparticle. The second is to evolve eco-friendly materials by using cellulose fibers as an alternative to advanced fibers in wood-plastic composites [1].

Reinforcing plastics with natural fibers has got numerous attractions mainly because of mechanical improvement that can be acquired at a relatively low cost [2]. Wood-polymer composites (WPCs) cover a wide extent of areas in the composite field. These are environmentally friendly, low cost consuming, renewable, and will restrain eco pollution by virtue of their component biodegradability, and they might a tremendous job in tackling the environmental issues that we might otherwise need to face within the future [3]. However, the possibility of reinforcement of natural fibers is greatly reduced due to their incompatibility and poor interfacial adhesion between organic polymer matrix and natural fibers. This ends up in poor miscibility among the ingredients and hence reduces the properties of the formed composites [4]. The compatibility between immiscible ingredients can be upgraded by utilizing suitable compatibilizers. The

✉ Alaa Bedir
  wpcfactory123@gmail.com

  Wagih Abdel Alim Sadik
  wagih_sadik@yahoo.com

  Abdel Ghaffar Maghraby El Demerdash
  eldemerd@yahoo.co.uk

  Rafik Abbas
  rafik.abbas@yahoo.com

[1] Department of Materials Science, Institute of Graduate Studies and Research, Alexandria University, 163 Horreya Avenue, Alshatby, Alexandria 21526, Egypt

compatibilizer like maleic anhydride grafted propylene (MAPP) or maleic anhydride grafted polyethylene (MAPE) improves the adhesion and miscibility between polymer matrix as hydrophobic part and natural fibers as hydrophilic part and at an identical time improves the surface interaction among totally different plastics [5, 6].

Rice husk, an unwanted agriculture residue in Egypt, is a by-product of the rice grinding industry. It is one of the most significant agricultural residues in the amount. It appears about 20% of the whole rice plant produced, on the weight basis of the rice plant. The evaluated annual rice husk waste production of 2.8 million tones in Egypt [7].

The consumption of organic thermoplastic has expanded enormously because of their various characteristics. The removal of plastic materials in the form of packaging films, bottles, etc. causes environmental pollution. The majority of the waste plastics comprise an essential amount of polyethylene (PE), polypropylene (PP), and polyvinyl chloride (PVC), etc. Recycling is the process of reusing to decrease the environmental pollution brought about by waste plastic materials and producing useful products. The utilization of recycled materials is limited because of their weak overall properties. These recycled plastics with poor properties are joined with natural fibers to form WPCs as a new product with promoted properties. The unconventional natural fibers can be changed into upgraded products by treating the waste thermoplastic products [8, 9].

Recently, nanotechnology has spread out a fresh out of the methodology for upgrading WPCs. By utilizing nanoparticles, the properties of achieved composites in the manufacturing field can be improved, making it possible to furnish new products with high-added value and additional potency improving the several properties of WPCs [10]. The most nanoparticles used nowadays are nanosilica and nanoclay that are widely utilized for these purposes. These nanoparticles are non-toxic, stable, relatively cheap, and available, display a layered morphology with a high aspect ratio, and massive surface area and cause an improvement within the properties of the WPCs. However, the hydrophilic nature of nanoclay and nanosilica obstructs the homogenous dispersion of nanoparticles in the hydrophobic polymer matrix due to incompatibility between them [11]. Modifying the surface of the nanoparticles through organic treatment will give a hydrophobic behavior to the surface of nanoparticles and enhance its compatibility with the hydrophobic polymer matrix [12]. In recent years, WPCs have pulled in extraordinary consideration in industrial applications. The main applications of WPCs in the world market include furniture, door board, door frame, wall panel, automotive, skirting, fences, siding, decking, air cleaner, and insulation mat manufacturing [13].

The principle goal of this study was to assess the capability of rice husk residues as a reinforcing agent for WPCs

Table 1 Chemical composition of the rice husk

Sample	Moisture (%)	Cellulose (%)	Hemicellulose (%)	Lignin (%)	Ash (%)
Rice husk	7% ± 0.4	35.5% ± 0.8	24.5% ± 1.9	22.6% ± 2.1	17.4% ± 3.3

Table 2 Basic characteristics of nanosilica and nanoclay

Properties	Nanosilica	Nanoclay
Physical state	Solid	Solid
Form	White powder	Off White powder
Organic modifier	Triethoxyvinylsilane	Hexadecyltrimethylammonium bromide
Density	2.2 g/cm^3	1.66 g/cm^3
Melting point/range	Approx. 1700 °C	Approx. 1750 °C
Thermal decomposition	> 2000 °C	> 2000 °C
SiO_2 content	> 99.8%	43.69%, Al_2O_3 (18.07%),
Particle size	15–20 nm	120 nm

so as to assay their efficiency. The effects of the addition of nanosilica to R-LLDPE/rice husk fibers composites and compared the findings with prepared composites based on nanoclay on the properties of prepared WPCs were investigated.

Materials and Methods

Materials

Recycled linear low-density polyethylene (R-LLDPE) with a melting temperature of 122.3 °C, melt flow rate of 0.9 g/10 min at 190 °C, and a density of 0.922 g/cm^3 was obtained by Prima Plast Egypt Company for plastic, Cairo, Egypt. Maleic anhydride grafted polyethylene (MAPE) as a coupling agent was supplied by BYK Additives & Instruments, German with a melting temperature at 134 °C, melt flow rate of 1.5 g/10 min at 190 °C, and density of 0.954 g/cm^3. Rice husk (RH) with 60–80 mesh size was collected locally in Alexandria, Egypt. The chemical composition of palm rachis fibers were analyzed by TAPPI test method, Chorination method and Kurschner- Hoffner method as presented in Table 1. Nanoclay (Sodium montmorillonite) modified with a quaternary ammonium salt with density 1.66 g/cm^3 was supplied from Nanoshel LLC, USA. Nanosilica (silicon dioxide) modified by triethoxyvinylsilane with density 2.2 g/cm^3 was obtained from Jiangsu XFNANO Materials, China. The specifications of the nanosilica and nanoclay are summed up in Table 2.

Preparation of Rice Husk Fibers

Rice husk (RH) was collected locally and was produced by a husking machine with exhausted shell separation. Small fibers were cleaned by drenching in distilled water for one day to evacuate any impurities on the surface fibers. Ground Fibers with high-speed blender were oven-dried at 80 °C for 24 h to adjust the content of moisture to less than 7% to get the best adhesion with polymer hence better formed WPCs and afterward stocked in sealed PE bags before sheet preparations.

Compounding and Sheet Preparation

Rice husk fibers (RH), recycled linear low-density polyethylene (R-LLDPE), and MAPE were mixed together and fixed at 65 wt%, 35 wt%, and 3 phc (per hundred compounds) respectively. These values were assigned according to the many professional manufactured formula and show a superb balance among execution and cost. The recycled linear low-density polyethylene (R-LLDPE), and MAPE were melted by a two-roll machine (Shaw Robinson Model 2799) using a melt blending process at 160 °C and 30 r/min for 3 min. At that point, RH fibers with different concentrations of nano-silica (NS) and nanoclay (NC) were incorporated into the blends for 10 min according to the formulations given in Table 3. WPCs sheets (350 mm*350 mm*4 mm) obtained by using compression molding (AUMYA) at 160 °C and 80 bar for 10 min.

Table 3 Composition of the studied formulations

Code	R-LLDPE (wt%)	RH (wt%)	MAPE (phc)	Nano-silica (phc)	Nan-oclay (phc)
R-LLDPE	100	0	0	0	0
WPC	35	65	0	0	0
WPC/M3	35	65	3	0	0
WPC/M3/NS2	35	65	3	2	0
WPC/M3/NS4	35	65	3	4	0
WPC/M3/NS6	35	65	3	6	0
WPC/M3/NC2	35	65	3	0	2
WPC/M3/NC4	35	65	3	0	4
WPC/M3/NC6	35	65	3	0	6

R-LLDPE recycled linear low-density polyethylene, *RH* rice husk, *MAPE* maleic anhydride grafted polyethylene, *phc* per hundred compounds

Characterization Techniques

Scanning Electron Microscopy (SEM)

SEM (JSM-5300, Japan) was used to characterize the morphology of the composites at 25 keV. The fractured surface of the samples was frozen under liquid nitrogen and coated with a gold layer (Au) to thickness of 400 Å (JFC-1100 E) to remove electron charging.

Fourier Transform Infrared Spectroscopy

Fourier transform infrared spectroscopic (FTIR) of nano-silica (NS), nanoclay (NC), and prepared composites were recorded on the FTIR spectrometer (Perkin-Elme, USA) in range of 4000 cm^{-1} to 500 cm^{-1} utilizing KBr disk.

Mechanical Property

The tensile properties (tensile strength and modulus) for R-LLDPE and prepared composites were estimated by utilizing a universal machine (Instron 4204, MA, USA) according to ASTM D 638-03. The test samples with Dumbbell-shaped were obtained by press cutting of the produced sheet. The tensile strength and modulus were obtained from the stress versus strain curves. At least five specimens were tested for each formulation. The flexural properties (flexural strength and modulus) were measured utilizing the three-point bending test method according to the ASTM D-790 method. The load was set midway among the supports. The bending test was led utilizing an Instron Universal Testing Machine (model 4486) at a speed of 2 mm/min.

The Izod impact strength of prepared samples was determined by utilizing a Zwick Universal Test Machine (model 5102) according to the ASTM D 256 test method. The prepared samples have a fixed dimension of 60*12*6 mm. five replicates specimens were tested for each formulation. obtained. The hardness of the specimens was determined according to the ASTM D2240 method utilizing a durometer (model RR12) and expressed as shore D hardness. The hardness value for each sample was calculated as the average of 5 measurements.

Thermal Property

The thermogravimetry (TG) and derivative thermogravimetry (DTG) of R-LLDPE/RH fibers composites with and without different nanoparticles (NS and NC) were determined utilizing a thermal analyzer (Shimadzu TGA-Q 50, Japan). The prepared samples (6 mg) were heated up to 600 °C at a heating rate of 20 °C/min under N_2 atmosphere to prevent the oxidation of the samples at a flow rate of 20 ml/min.

Differential scanning calorimetry (DSC) of the prepared composites was investigated utilizing the DSC calorimeter (Shimadzu-60 A, Japan). The samples (6 mg) were sealed in an aluminum pan and heated up to 300 °C at a heating rate of 10 °C/min under N_2 atmosphere at a flow rate of 20 ml/min.

Physical Property

Water absorption and thickness swelling testing were measured according to ASTM D 570-98 method. The WPC specimens were immersed in distilled water for a period of time at ambient temperature. At the end of immersion time, WPC samples were ejected from the distilled water and excess water on the surface of samples was wiped by tissue paper. The values of the water absorption (WA %) were calculated using the equation.

$$WA~(\%) = \frac{M_2 - M_1}{M_1} \times 100$$

where M_1 is the dry initial weight, M_2 is the weight of the sample after immersion in water. Also the values of the TS in percentage were calculated using the following equation

$$TS~(\%) = \frac{T_2 - T_1}{T_1} \times 100$$

where T_1 is the initial thickness of the sample and T_2 is the thickness of the wetted sample.

Results and Discussion

Role of MAPE in the Compatibility Between Polymer and Natural Fiber

The efficiency of the natural fibers/thermoplastic interface is considerable for the use of cellulose fibers as reinforcing agents in the fabrication of WPCs. The composites properties rely upon all of the individual ingredients and on their interfacial adhesion. The main obstacle in WPCs fabrication is the incompatibility between polar natural cellulose fiber and nonpolar polymer matrix. This problem can be relieved by the utilization of compatibilizers such as maleic anhydride grafted polyethylene (MAPE). This compatibilizer has double features in that it has the hydrophobic and hydrophilic properties together wanted to cohere well with the hydrophobic polymer and react with the hydrophilic natural fibers [5, 14].

Thus, covalent bonds are formed between the hydroxyl groups located on the surface of natural fibers and the compatibilizer in the form of the ester bond. In addition, the hydrogen bonds might likewise participate in interaction as shown in Fig. 1. From that mechanism, MAPE should improve the properties of the composite by promoting interfacial adhesion between the phases besides the good dispersion of natural fibers as well [15].

Morphological Analysis

SEM Study

SEM was used to investigate the morphology and the possible interfacial adhesion between the R-LLDPE matrix and its composites. Figure 2 shows SEM micrographs taken from the fracture surface of samples broken during the tensile tests for the studied composites and WPCs loaded with different nanoparticle contents (2, 4, and 6 phc). SEM micrographs of R-LLDPE only are shown in Fig. 2a; it can be observed homogeneous dispersion of R-LLDPE in a matrix. Figure 2b shows the agglomeration of RH fibers and some holes and cavities in the surface that have a negative effect on the water absorption and mechanical properties [16]. This shows that the efficiency of interaction bonding between the rice husk fibers (RH) and R-LLDPE matrix is weak, so when stress is applied, it causes RH fibers to be pulled out from the R-LLDPE and leaving behind holes easily. Figure 2c shows the effect of compatibilizer (MAPE) on the R-LLDPE/RH fibers composite. The number of holes and cavities are decreased and the adhesion between RH fibers and R-LLDPE matrix is improved due to the formed the covalent and hydrogen bond as explained and stated earlier in Fig. 1. Figure 2d–f shows the impact of the addition of nanosilica contents (2, 4, and 6 phc) respectively on the prepared composites. The addition of nanosilica showed uniform homogenous dispersion of the nanosilica within the R-LLDPE, and there are no RH fibers were pulled out. This confirmed that majority of the nanosilica have dispersed and filled the cavities at the interface between R-LLDPE and RH fibers, components which demonstrated a more interaction bond among the nanosilica, RH and the R-LLDPE [17].

Figure 2g and h shows The effect of addition of nanoclay contents (2, and 4 phc) respectively on the composites showed homogenous dispersion on nanoclay pellets in R-LLDPE, but the impact of the addition of nanoclay with a high concentration (6 phc) on the morphology of the prepared composites is illustrated in Fig. 2i. An evident nanoclay layers agglomeration was seen in the prepared composite with high nanoclay content. This resulted in an ease of nanoclay layers to pull out from the polymer and leaving behind small holes, where the agglomeration of the nanoclay pellets in the R-LLDPE occurs because of the high surface area of nanoclay layers and Van der Waals forces between them. Thus, during the blending of the nanoclays with R-LLDPE matrix, just a slight amount of the polymer matrix can permeate among the agglomerated layers of nanoclay and interact with them, thereby reducing the interfacial
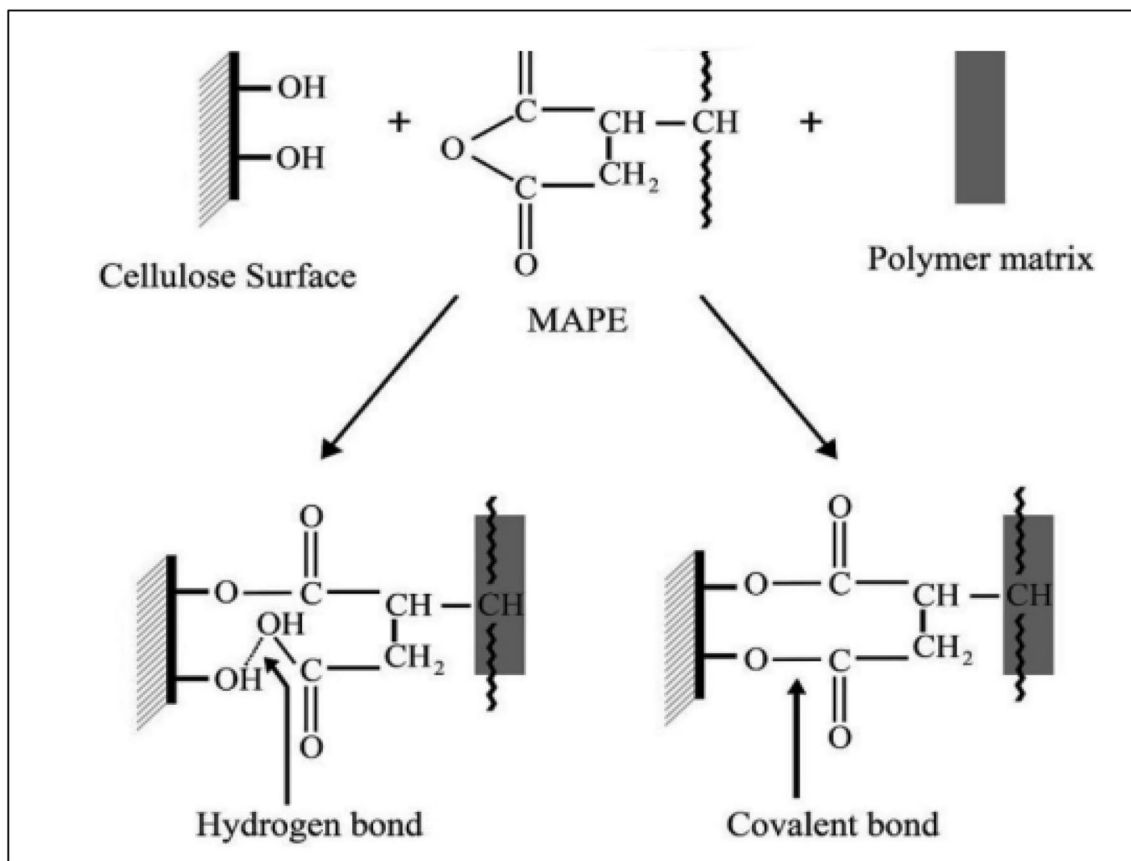
Fig. 1 Schematic represented the reaction between cellulose fiber hydroxyl end groups and maleic anhydride grafted polyethylene (MAPE)

adhesion between the nanoclay layers and the polymer [18, 19].

FTIR Results

Figure 3a shows the FTIR spectra of nanosilica (SiO$_2$). Some absorption peaks at 3486 cm^{-1} for –OH stretching, 2931 cm^{-1} for –CH stretching of modified hydrocarbon, and 1632 cm^{-1} for –OH bending of hydroxyl group adsorbed on the surface of nanoparticles. The other peaks appeared in the range 1187–465 cm^{-1} was due to Si–O–Si group in the SiO$_2$. However, nanoclay exhibited the peaks at 3542 cm^{-1} for –OH stretching, 2927 cm^{-1} for –CH stretching of modified hydrocarbon, 1629 cm^{-1} for –OH bending, and 1031–460 cm^{-1} (oxide bands of metals like Si, Al, Mg, etc.) as shown in Fig. 3b [20, 21].

Figure 4a shows FTIR spectra of R-LLDPE in which, bands at 2947 cm^{-1} and 2877 cm^{-1} are due to asymmetrical and symmetrical C–H stretching vibrations. The band at 1375 cm^{-1} is from CH$_3$ symmetric vibrations and the absorbance bands at 1456 cm^{-1} and 921 cm^{-1} are associated with vibrations of CH$_2$ from the polyethylene chain.

The nature of adhesion between rice husk fibers and R-LLDPE matrix was explored using FTIR spectroscopy [22]. Figure 4b and c shows the FTIR spectra of studied composites with and without compatibilizer (MAPE). MAPE can be bonded to the rice husk fibers surface by ester linkage and hydrogen bonds. The shifting of absorption peak corresponding to hydroxyl group to lower wavenumbers 3257 cm^{-1} affirmed the forming of hydrogen linkage between RH fibers and R-LLDPE. Moreover, the intensity of peaks at 2936 cm^{-1} corresponding to –CH stretching was more in wood-plastic composites compared to uncompatibilized composites which demonstrated the bond formed between R-LLDPE, MAPE, and RH fibers. The effect of addition nanosilica, and nanoclay was appeared by FTIR, where the decrease in intensity of –OH groups in the nanocomposite might be related to chemical modification with nanosilica and nanoclay where the silica particles replaced the hydrogen atom in –OH groups to produce Si–O–Si stretched vibration that reduced the intensity of –OH groups. Si–O–Si stretched vibration as confirmed by peaks at 1082 and 1024 cm^{-1} as shown in Fig. 4d and e [23].
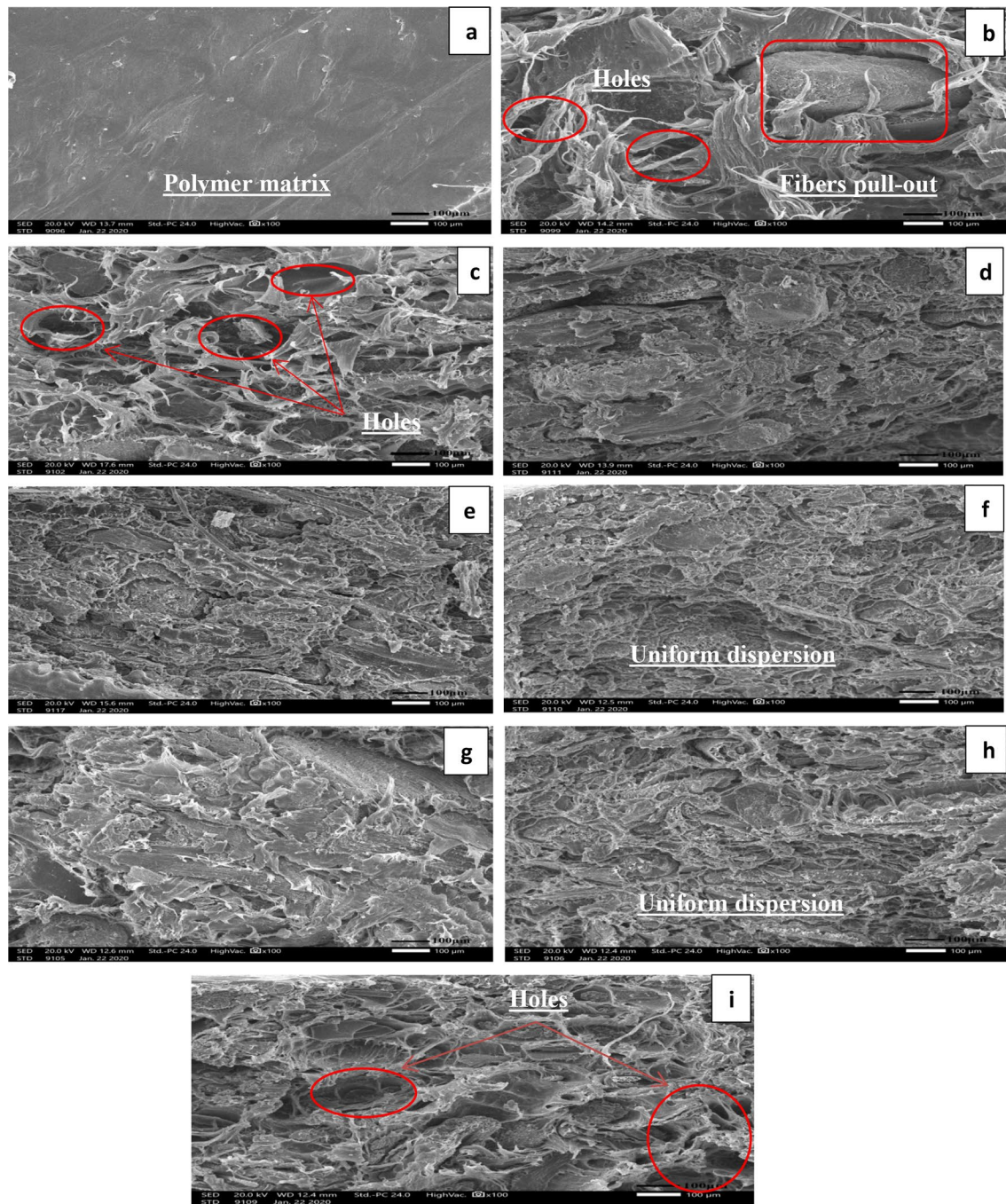
Fig. 2 SEM micrographs of fractured surfaces of the studied composites: **a** R-LLDPE, **b** WPC, **c** WPC/M3, **d** WPC/M3/NS2, **e** WPC/M3/NS4, **f** WPC/M3/NS6, **g** WPC/M3/NC2, **h** WPC/M3/NC4, and **i** WPC/M3/NC6

Mechanical Properties

Tensile Properties

Figure 5 shows the tensile strength of studied composites at different nanosilica and nanoclay loadings. The tensile strength of the uncompatibilized R-LLDPE/RH fiber composites decreased from 13.7 to 5.34 MPa with the incorporation of RH fibers at 65 wt%. The reduction of tensile strength might be due to poor adhesion between rice husk fibers and R-LLDPE matrix. In addition, the other reason was the irregular shape of the natural fibers, because their capability to support stress transmitted from the polymer is rather poor. The decrease in tensile strength may be also clarified because of the agglomeration of natural fibers and the dewetting of the polymer

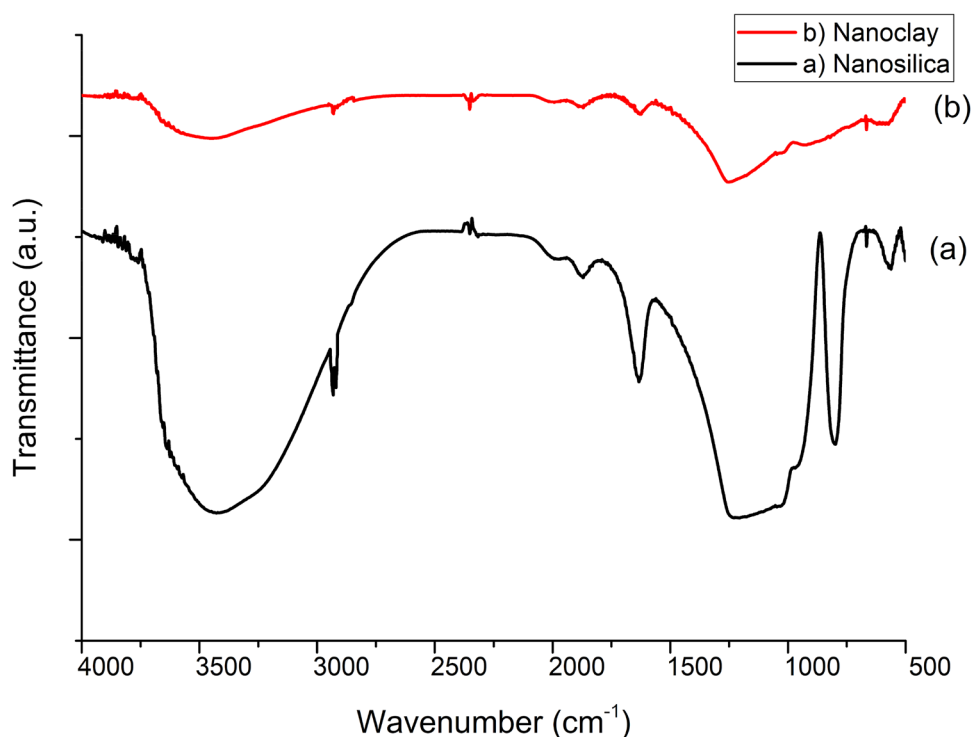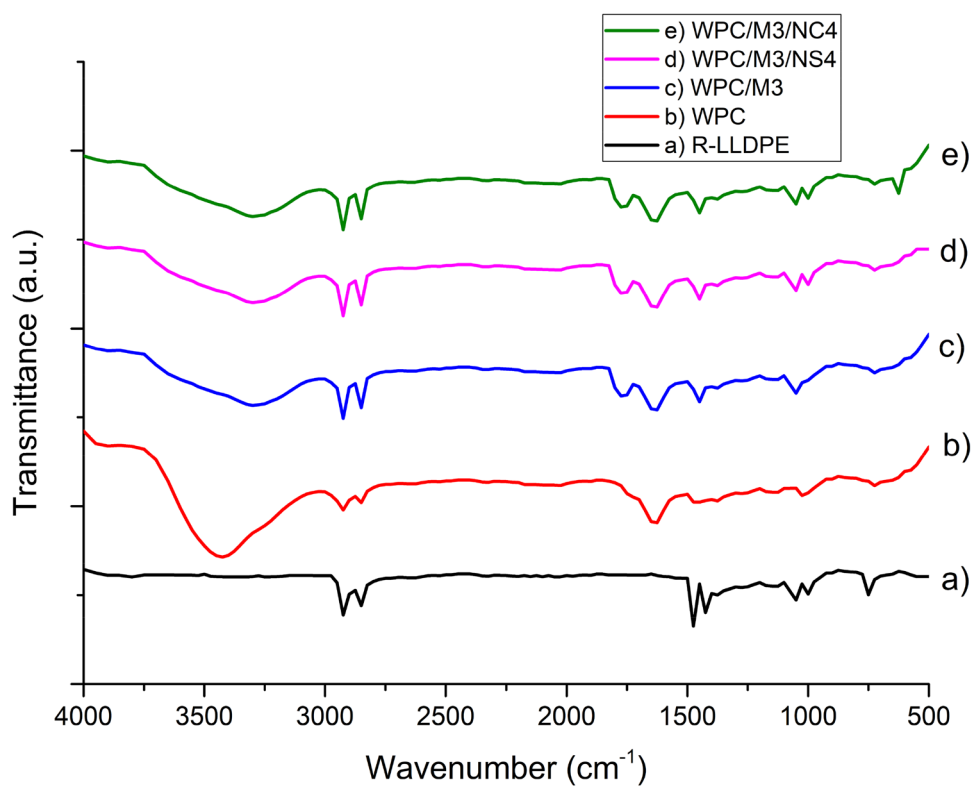**Fig. 3** FTIR spectrum of nano-silica and nanoclay

Fig. 4 FTIR spectra of *a* R-LLDPE, *b* WPC, *c* WPC/M3, *d* WPC/M3/NS4, and *e* WPC/M3/NC4

at the interphase. The addition of MAPE showed high tensile strength for R-LLDPE/RH composites compared to uncompatibilized composites [24]. The results could be clarified as far as good interaction at R-LLDPE/RH interface, due to the activity of MAPE. The interfacial adhesion was evolved by hydrogen linkages formed between the hydroxyl groups on the surface of RH fiber and compatibilizing agent [25, 26].

Fig. 5 Tensile strength of the studied composites
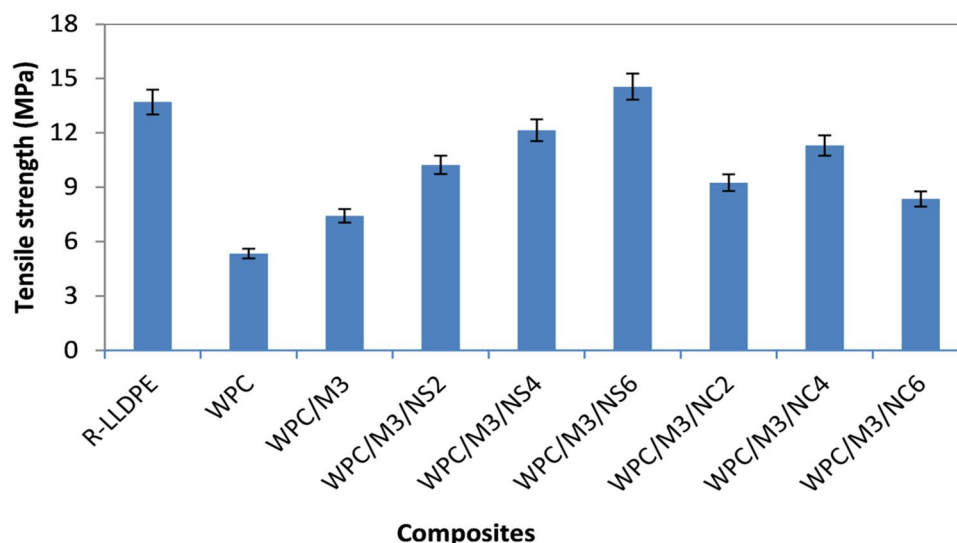
Addition of nanosilica at (2, 4, and 6 phc) contents improved the tensile strength of prepared composites by 38%, 63.8%, and 76.1%, respectively. This increase might due to the improvement in the surface area for interaction between nanosilica and polymer matrix which depends on the uniform dispersion of silica nanoparticles in the R-LLDPE [27]. In contrast, the incorporation of nanoclay at (2 and 4 phc) improved the tensile strength of composites by 24.6%, and 52.4, respectively. The addition of nanoclay layers at (2 and 4 phc) increased the tensile strength of prepared WPCs by 24.6%, and 52.4, respectively. the enhancement in tensile strength of treated composites with nanoclay due to the high aspect ratio and the uniform dispersion of nanoclay pellets in the R-LLDPE matrix, whereas, the addition of high concentration of nanoclay (6 phc) decreased the tensile strength by 35.3%. Reduction in tensile strength

is most likely because of the accumulation of the nanoclay (NC) layers which drastically reduces the dispersion of the nanoparticles in the polymer matrix [28, 29].

Figure 6 shows the tensile modulus of prepared composites. The tensile modulus of the uncompatibilized R-LLDPE /RH fiber composites increased from 311 to 679 MPa with the incorporation of RH fibers. The improvement in tensile modulus might be due to improve the stiffness of studied composites because of the higher stiffness of RH fibers than R-LLDPE matrix and hence add stiffness to the composites [15]. The addition of MAPE showed high tensile modulus for R-LLDPE/RH composites indicating a homogenous distribution of RH fibers and better fiber-matrix interaction. The addition of nanosilica at (2, 4, and 6 phc) contents improved the tensile modulus of prepared composites by 11.8%, 22.2%, and 36.3%, respectively. The improvement

Fig. 6 Tensile modulus of the studied composites
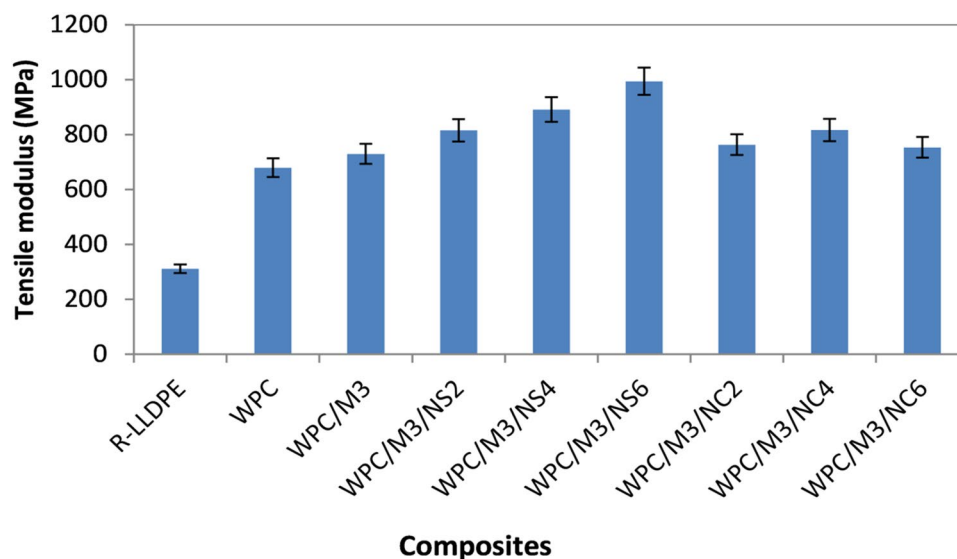
in the properties of treated composites due to the higher stiffness of silica nanopartices than other ingredients in the composites. In addition, the influence of restriction in the mobility of polymer chain and increase in adhesion caused significant enhancement in mechanical properties. On the other hand, the incorporation of nanoclay at (2, 4 phc) contents improved the tensile modulus of prepared composites by 6.2%, and 12.1, respectively. Tensile modulus decreased at the addition of nanoclay 6 phc by 8.4%. Reduction in tensile modulus is probably because of the agglomeration of the nanoclay layers [30, 31].

Flexural Properties

Figure 7 shows that the trend of flexural properties of the studied composites as a function of nanosilica and nanoclay content was similar to that of tensile properties discussed earlier. The flexural strength of R-LLDPE/RH fiber composites without MAPE reduced from 16.54 to 7.03 MPa with the incorporation of RH fibers at 65 wt%. The reduction of flexural strength might be due to fibers aggregation takes place where polymer matrix in composites acts as an adhesive for binding RH fibers together. So obviously increasing the loading of RH fibers and decreasing the quantity of R-LLDPE matrix causes a decline owing to poor interfacial adhesion among fibers and the R-LLDPE polymer leads to a stress concentration around the RH fibers. Plus, higher natural cellulose fibers content results in more and much most likely void formation during fabrication thusly reduces the flexural properties [8]. The addition of MAPE improved flexural strength for R-LLDPE/RH composites. Similar to the tensile properties, the addition of nanosilica at (2, 4, and 6 phc) contents to R-LLDPE/RH fibers composites improved the flexural strength by 16.45%, 31.4%, and 56.1%, respectively. In contrast, the incorporation of nanoclay at (2 and 4

phc) to R-LLDPE/RH fibers composites improved the flexural strength of composites by 7.4%, and 25.9, respectively. But, the addition of a high concentration of nanoclay and (6 phc) decreased the flexural strength, due to the agglomeration/clogging of the nanoclay layers [32, 33].

Figure 8 shows the flexural modulus of studied composites at different nanosilica and nanoclay loadings. The flexural modulus of the uncompatibilized R-LLDPE/RH fiber composites increased from 208 to 628 MPa with the incorporation of RH fibers at 65 wt%. The addition of MAPE showed high flexural modulus for R-LLDPE/RH composites compared to uncompatibilized composites. Incorporation of nanosilica at (2, 4, and 6 phc) contents to R-LLDPE/RH fibers composites improved the flexural modulus by 14.3%, 23.5%, and 40.4%, respectively, and to R-LLDPE/PR fibers composites improved by 14.9%, 27.3%, and 39.2%, respectively. In contrast, the incorporation of nanoclay at (2 and 4 phc) to the prepared composites improved the flexural modulus of composites by 5.9%, and 17.4, respectively. Composites with the addition of a high concentration of nanoclay (6 phc) decreased the flexural modulus, due to the agglomeration of the nanoparticles [1, 34].

Impact Strength

Figure 9 shows the impact strength of the prepared composites. The izod impact strength of the composites without MAPE decreased from 22 to 12.48 kJ/m^2 with the incorporation of RH fibers at 65 wt%. The reduction in impact strength might be due to weak interaction among the RH fibers and polymer matrix causes micro-crack to occur at the point of impact, which causes the cracks to effectively propagate in the prepared composite. These micro-cracks cause reduced impact strength of the composites. The addition of MAPE showed did not improve

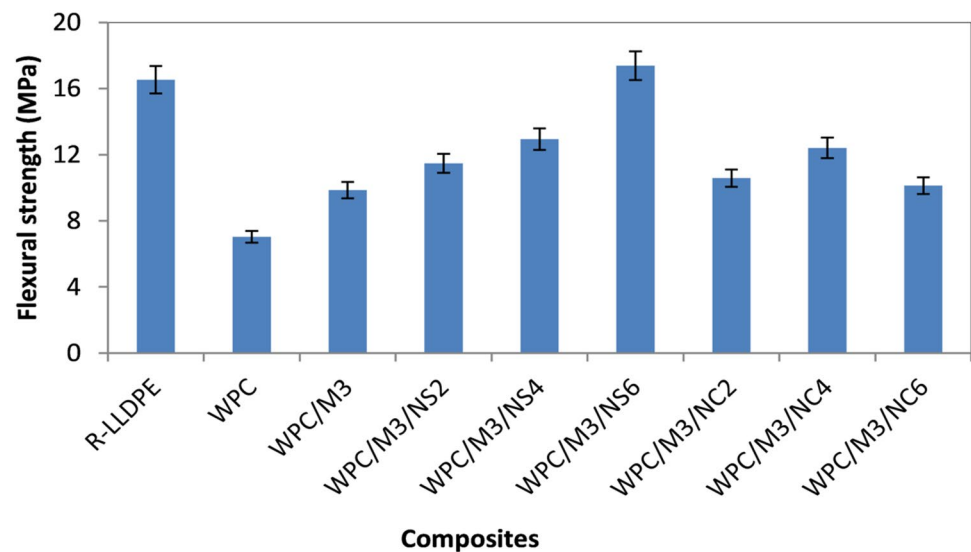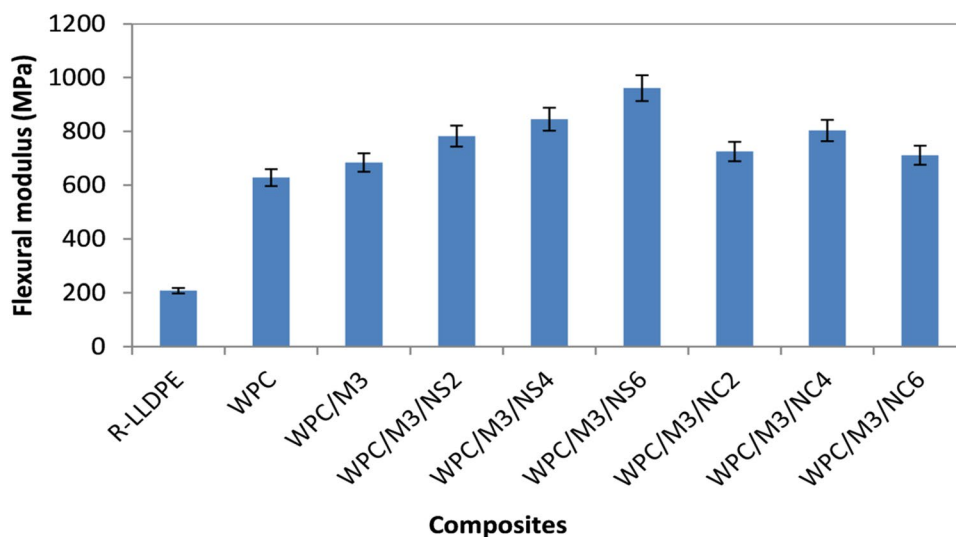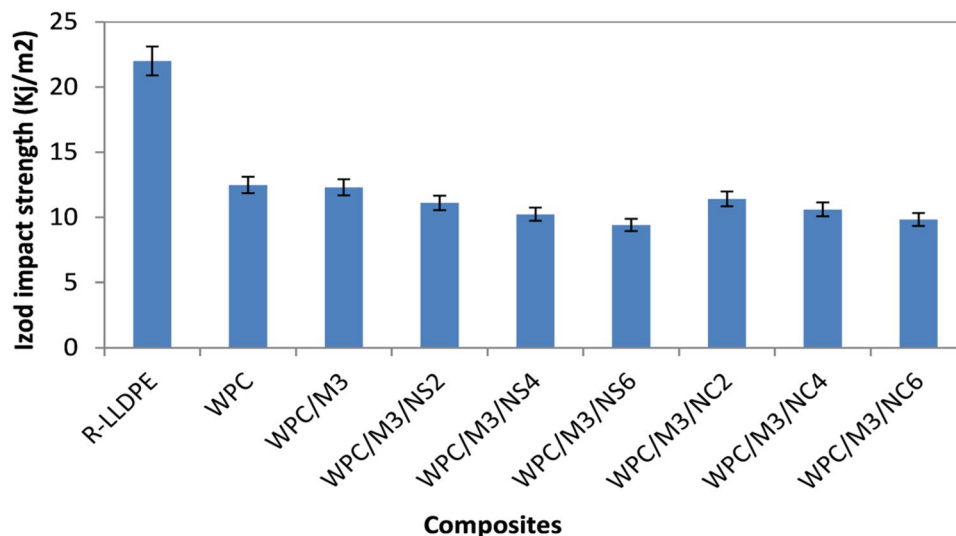**Fig. 7** Flexural strength of the studied composites

Fig. 8 Flexural modulus of the studied composites

**Fig. 9** Izod impact strength of the studied composites

the impact strength for WPCs, where the interfacial bonding between RH fibers and R-LLDPE matrix was highly improved, thus the micro-crack was not started at the interface, but at the RH fiber itself, when the izod impact occurred. The RH fibers is more brittle than the R-LLDPE matrix, and this causes decreased izod impact strength in the prepared composites [15, 35].

Also, the impact strength was diminished by the addition of different nanoparticles (NS or NC) in the WPCs. The deterioration in impact strength might because of the impact of NS and NC particles in the R-LLDPE supplys points of stress concentrations, thus giving sites for crack initiation. Also, another cause for a decline of impact strength might be the stiffening of the chain of R-LLDPE matrix which result in less efficiency to absorb impact energy [36].

Hardness

Figure 10 shows the hardness (shore D) of studied composites at different nanosilica and nanoclay loadings. The hardness of the uncompatibilized composites increased from 46 to 58.5 with the incorporation of RH fibers at 65 wt%. The enhancement in hardness might be due to improve the stiffness of prepared composites because of the higher stiffness of RH fibers and a decrease in mobility of polymer chain (brittle behavior). This implied that the incorporation of natural fibers diminished the ductility of the composites, where polymer matrix mobility or deformability of a rigid interface between the fiber and the matrix decreased leading to a brittle failure under loading. The additions of MAPE showed a slight improvement in the hardness from 58.5 to 60.4. The addition of nanosilica at (2, 4, and 6 phc) to R-LLDPE/RH

Fig. 10 Hardness of the studied composites
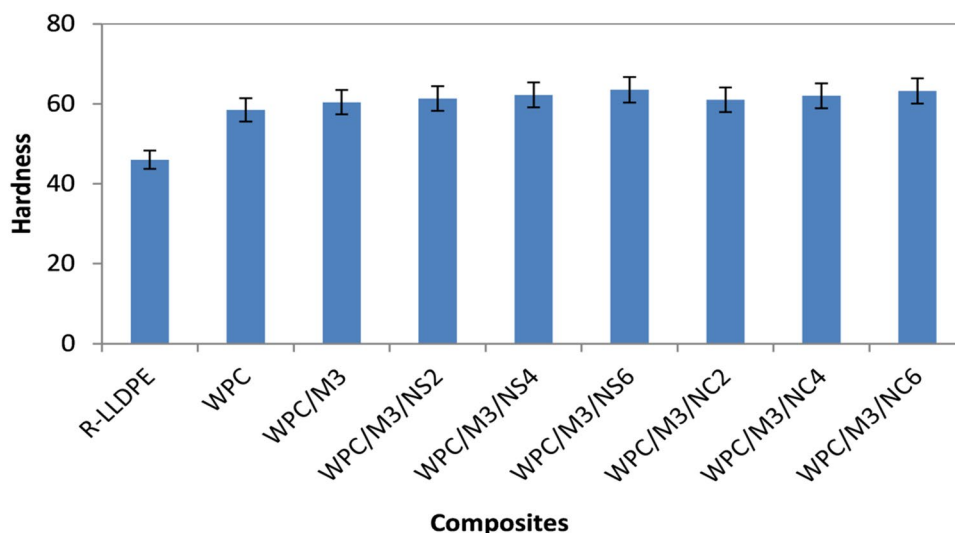
fibers composites slightly increased hardness by 1.45%, 3%, and 5.1%, respectively. Also, incorporation of nanoclay at (2, 4, and 6 phc) to R-LLDPE / RH fibers composites slightly increased the hardness by 0.99%, 2.65%, and 4.6%, respectively. The reason for increase in hardness values could be explained and stated earlier [37, 38].

Thermal Properties

TGA Analysis

The impact of addition of nanosilica (NS) and nanoclay (NC) on the thermal behavior of the studied composites was investigated utilizing TGA. Figure 11 shows the thermogravimetry (TG) and derivative thermogravimetry (DTG) curves for all prepared composites with different nanoparticle loading. The thermal behavior of the prepared composites is summed up in Table 4. The degradation of R-LLDPE began at about 399 °C, and the maximum decomposition rate appeared at about 473 °C. It was seen that the thermal degradation curve of all prepared WPCs was divided into two main stages of thermal degradation of mass loss at about: and 392 to 502 °C. The first stage which contained the range 248 to 362 °C had a maximum degradation temperature (T_{max}) at 302 °C due to the degradation of the components of RH fibers like lignin, cellulose, and hemicellulose, while another stage with range 392 to 502 °C had maximum degradation temperature (T_{max}) at 473 °C is attributed to the pyrolysis of R-LLDPE [39]. The results indicated that the addition of NS and NC slightly increased the thermal stability of the prepared composites by 3–7 °C. The most fundamental think thermal stability, which has been formed by different nanoparticles (NS or NC), is that the producing of a char layer that is non-burning; ultimately, the high specific surface area and proper coverage of the char layer

affect thermal property. Also, the incorporation of NS and NC particles lead to the formation of the crystal structure in the prepared composites. These features improve the thermal degradation temperature of the studied composites and increase their thermal property. In addition, the strong interaction among the R-LLDPE, RH fibers and nanoparticles (NS or NC) play important role in improving the thermal stability of WPCs [28, 40].

DSC Analysis

DSC tests were proceeded to describe the thermal stability of the R-LLDPE and the R-LLDPE/RH fiber composites. The melting enthalpy (H_m) and melting temperature (T_m) of the prepared composites were summed up in Table 4. A single endothermic melting curve was monitored for all prepared WPCs. It was seen that the incorporation of nanoparticle (NS or NC) didn't show a striking variation in the values of melting temperature (T_m) of the prepared composites. The values for Tm stayed comparatively consistent for all prepared WPCs, changing from 118.6 to 122.3 °C. This indicated that in the existence of RH fibers and different nanoparticles (NS or NC), the size of the crystalline domains was held in the WPCs, The melting enthalpy (H_m), however, diminished with the RH fibers increasing loading, as expected, due to the reduction in the amount of R-LLDPE [41]. The degree of crystallinity (X_c) of the composites decreased from 41.24% to 24.76% with incorporation of RH fibers. This meant that the RH fibers did not act as a nucleating agent in this composite system. The reason for the reduction of the X_c of the composite should be attributed to the disturbance in the crystalline formation induced by the RH in the composite during the cooling process. The degree of crystallinity (X_c) of the WPCs increased by 9–15% with the addition
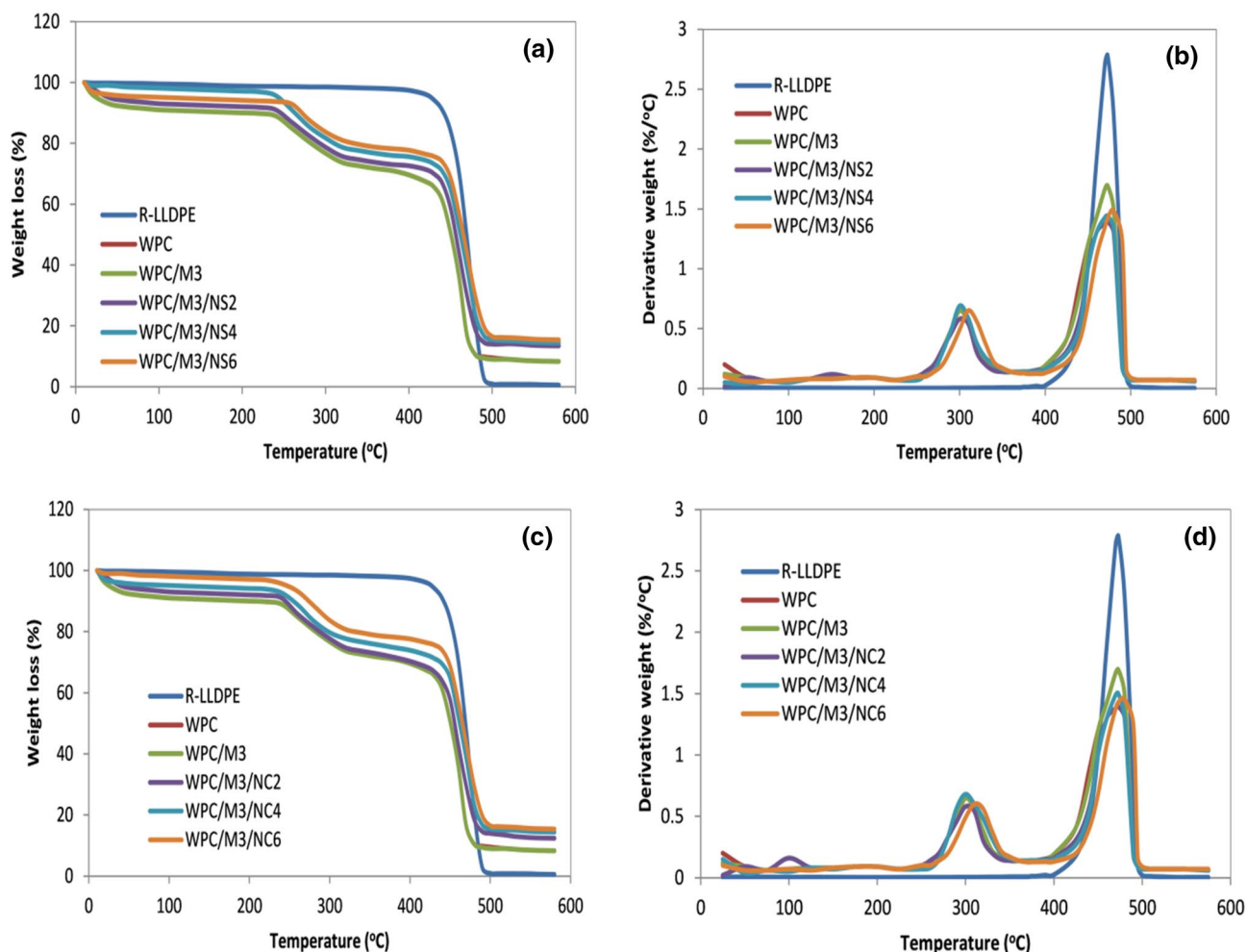
Fig. 11 TG (**a**, **c**) and DTG (**b**, **d**) curves for the studied composites with different nanoparticles content

Table 4 Thermal properties of the composites with different nanoparticles contents

Sample	First stage		Second stage		T_m (°C)	H_m (J/g)	X_c (%)
	$T_{(range)}$ (°C)	$T_{(max)}$ (°C)	$T_{(range)}$ (°C)	$T_{(max)}$ (°C)			
R-LLDPE	–	–	399–498	473	122.3	158.82	41.24
WPC	248–352	302	392–495	473	119.4	69.73	24.76
WPC/M3	249–352	301	396–498	472	119.1	69.63	25.54
WPC/M3/NS2	251–354	302	398–499	473	118.6	68.12	34.27
WPC/M3/NS4	254–355	303	398–500	474	121.4	69.03	36.57
WPC/M3/NS6	260–362	309	401–502	478	120.7	68.82	40.38
WPC/M3/NC2	250–354	302	397–498	473	119.8	68.43	33.41
WPC/M3/NC4	252–353	301	397–501	473	122.1	69.25	36.45
WPC/M3/NC6	259–361	309	401–502	477	120.4	69.69	30.23

of nanosilica and nanoclay. This result may be due to the nucleating effect of the NS and NC that could provide heterogeneous nuclei during the initial nucleation stage for the crystallites, which increased the crystallinity of the WPCs. Moreover, the addition of silica particles increased

the crystallization temperature, which confirmed that in the presence of NS and NC, crystals formed sooner. This phenomenon played a role in the enhancement of the capability of creating crystallized nuclear and the stimulation of crystal creation within the polymer matrix [42].

Physical Properties

Water Absorption

Water absorption or water uptake is one the most important parameters should be taken into consideration for the fabrication of wood-plastic composites (WPCs) since it the effect on the dimensional stability and the mechanical properties of WPCs. Figure 12 shows The impact of the incorporation of different nanoparticles (NS or NC) on the water absorption observed in the prepared WPCs after 15 days of water immersion times. Generally, the water absorption of prepared composites increases dramatically with the increasing amount of natural cellulose fibers and increasing immersion time [43]. The enhancement in water absorption of R-LLDPE/RH fibers composites because of the hydrophilic behavior of RH fibers, this related to the hydrogen linkages formed between the hydroxyl groups on the surface RH

fibers (cellulose and hemicellulose) and water molecules. Additionally, the penetration of water molecules in RH fibers by the capillary action due to the massive amount of porous tubular structures found in the natural cellulose fibers. Mechanism of water absorption in very WPCs embodies capillary action through natural cellulose fibers, diffusion through the R-LLDPE, or diffusion at the interface between RH fibers and R-LLDPE. Therefore, water uptake depends not solely on the hydrophilic behavior of the RH fibers and the R-LLDPE yet also on interfacial adhesion between them (gaps) [44].

The time consumed to arrive in the saturation state was the same for all the prepared WPCs as observed in the present study. The water absorption of the pure R-LLDPE, however, was less than 0.2%, due to its hydrophobic nature. And, we found that water absorption of treated composites with compatibilizer is lower than that of untreated composites. Due to the quantity of –OH groups

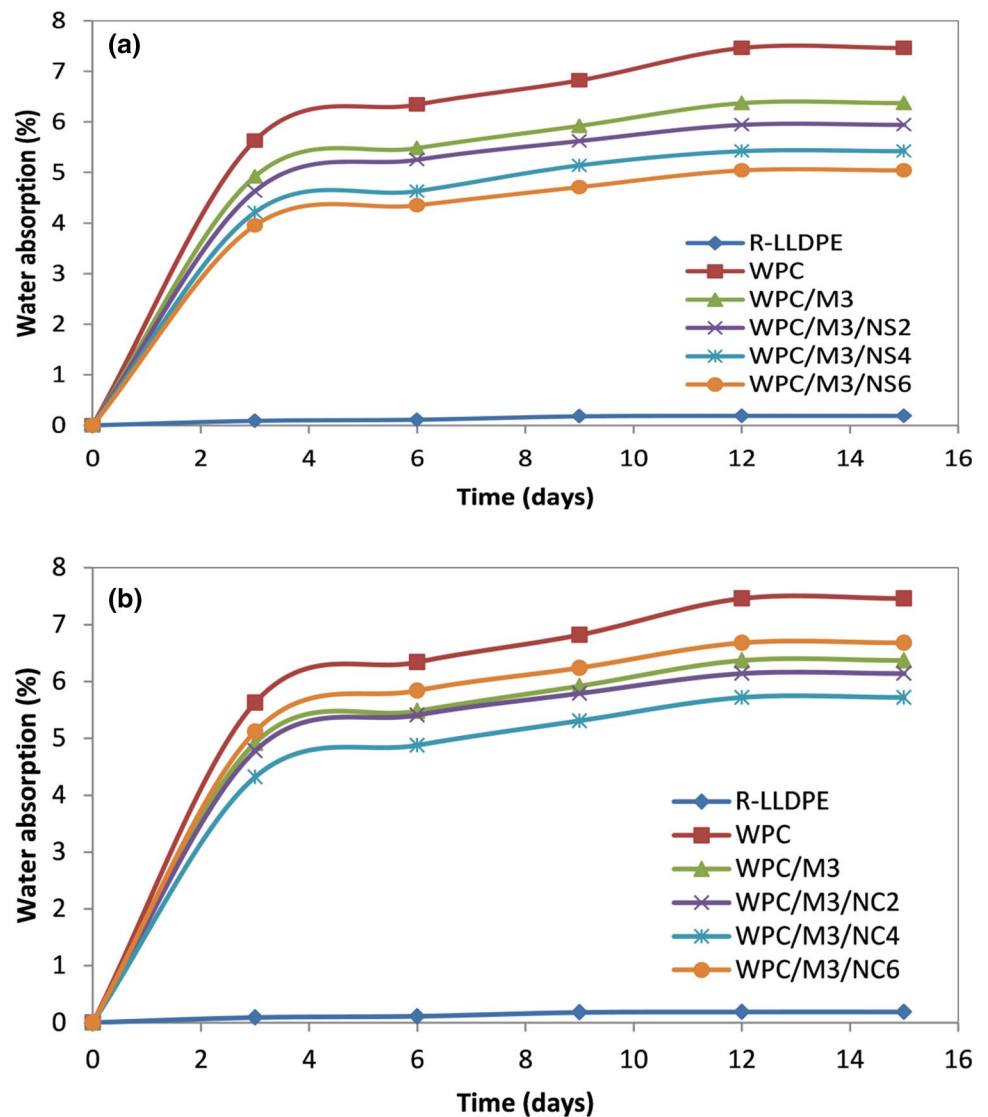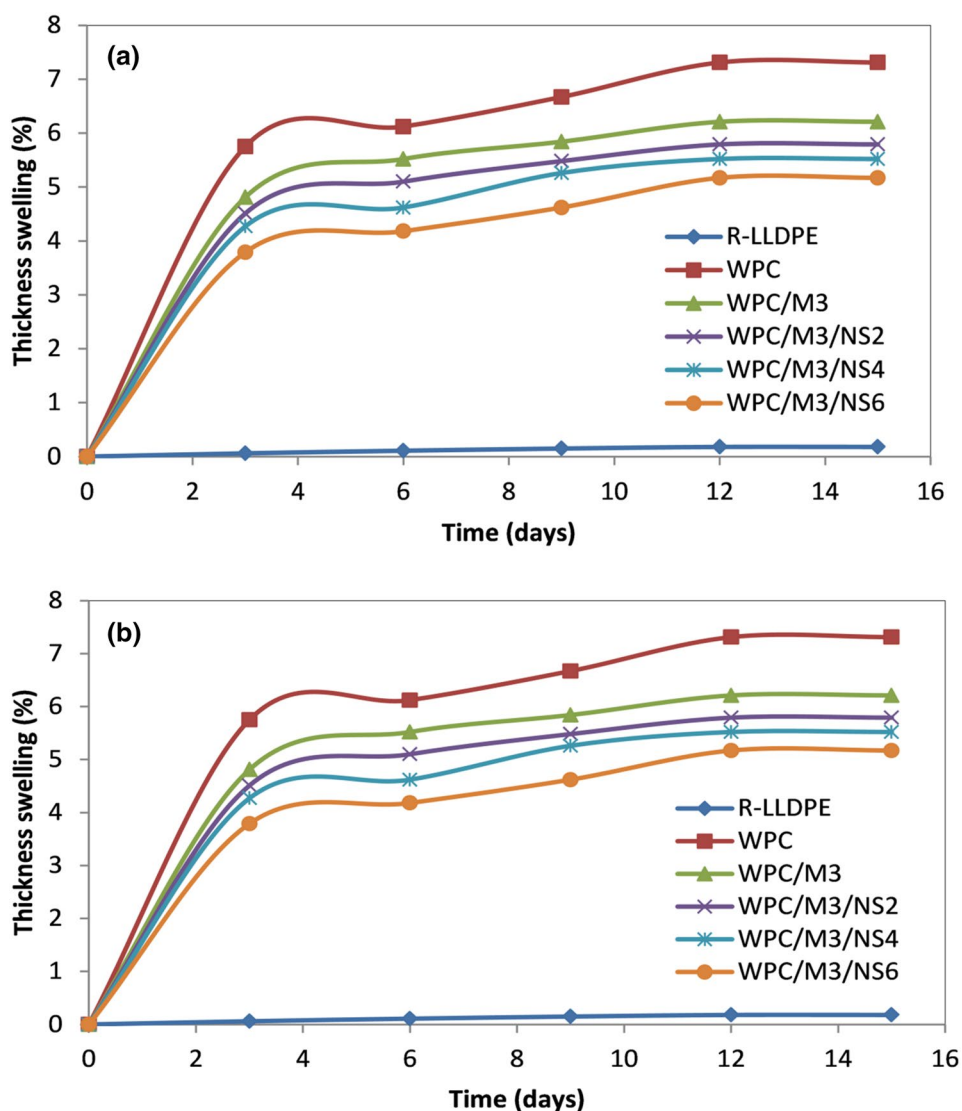**Fig. 12** Water absorption of the studied composites

Fig. 13 Thickness swelling of the studied composites

could be diminished via the esterification between MAPE and –OH of rice husk fibers. Therefore, water uptake got limited. Also, the gaps in treated WPCs by compatibilizer were less due to the amelioration of interfacial adhesion of RH fibers/R-LLDPE composites, which restricted the penetration of water molecules into the prepared WPCs. In addition, the incorporation of nanosilica at (2, 4, and 6 phc) decreased the water absorption after 12 days by 4.65%, 11.4%, and 21.81%, respectively, due to NS particles act as a barrier or water repellent where they have a high surface area so it well dispersed in the prepared composite and improves interfacial adhesion causes a decrease of the voids and decreases penetration of the water molecules into the prepared WPCs. In contrast, incorporation of nanoclay at (2, and 4 phc) decreased the water absorption by 3.8% and 8.76%, respectively, the addition of high content (6 phc) increased again the water absorption by 4.03% due to the aggregation of the NC layers [45, 46].

Thickness Swelling

Figure 13 shows thickness swelling of the studied composites after 15 days of immersion in distilled water. The thickness swelling of the prepared WPCs increases with the water uptake and in this manner has a trend sort of like that of the water absorption. It can be seen that the prepared WPCs without different nanoparticles (NS or NC) showed the most elevated thickness swelling values. By the addition of NS and NC particles, the thickness swelling decreased due to the same reasons as discussed concerning water absorption. The higher the nanoparticle content, the lower was the thickness swelling [16, 47].

Conclusions

The present work showed that rice husk fibers can be successfully utilized to make R-LLDPE/rice husk composites with helpful physico-mechanical properties. The findings of the research demonstrated that the SEM study indicated improved the interaction between the ingredients resulting in decreased numbers of cavities and pulled-out RH fibers with the addition of nanosilica (up to 6 phc) and the addition of nanoclay (up to 4 phc) would behave the same behavior. However, adding nanoclay (6 phc) didn't improve these properties. This was related to the agglomeration and weak dispersion when a high amount of nanoclay was used, which resulted in increased gaps and cracks in the prepared WPCs. It was found that increasing the nanosilica and nanoclay content up to 6 phc and 4 phc respectively, led to enhance tensile and flexural strength as well as tensile and flexural modulus of prepared composites. Izod impact strength was decreased by the incorporation of different nanoparticles in contrast with the hardness. These properties were reduced by incorporation of 6 phc nanoclay. The physical properties of composites were lowered with the increased nanosilica and nanoclay content. The thermal stability of WPCs slightly improved according to the impact of different nanoparticles (NS, and NC). At long last, the Utilization of reused plastics and rice husk fibers in composites have several benefits such as limit the solid waste content and conserve natural resources. In addition, the utilization of nanoparticles in recycling agricultural and solid waste to developing wood plastic composites (WPCs) by improving their properties for a wide range of applications.

References

1. Zahedi M, Khanjanzadeh H, Pirayesh H, Saadatnia MA (2015) Utilization of natural montmorillonite modified with dimethyl, dehydrogenated tallow quaternary ammonium salt as reinforcement in almond shell flour–polypropylene bio-nanocomposites. Compos B Eng 71:143–151
2. Lei Y, Wu Q, Yao F, Xu Y (2007) Preparation and properties of recycled HDPE/natural fiber composites. Compos A Appl Sci Manuf 38(7):1664–1674
3. Yang X, Tang X, Ma L, Sun Y (2019) Sound insulation performance of structural wood wall integrated with wood plastic composite. J Bioresour Bioprod 4(2):111–118
4. Anbupalani MS, Venkatachalam CD, Rathanasamy R (2020) Influence of coupling agent on altering the reinforcing efficiency of natural fibre-incorporated polymers–a review. J Reinf Plast Compos. https://doi.org/10.1177/0731684420918937
5. Raj R, Kokta BV, Maldas D, Daneault C (1989) Use of wood fibers in thermoplastics. VII. The effect of coupling agents in polyethylene–wood fiber composites. Journal of Applied Polymer Science 37 (4):1089–1103
6. Han G, Lei Y, Wu Q, Kojima Y, Suzuki S (2008) Bamboo–fiber filled high density polyethylene composites: effect of coupling treatment and nanoclay. J Polym Environ 16(2):123–130
7. Ibrahim MIM, Mohamed NAEM (2016) Towards sustainable management of solid waste in Egypt. Proc Environ Sci 34:336–347
8. Turku I, Keskisaari A, Kärki T, Puurtinen A, Marttila P (2017) Characterization of wood plastic composites manufactured from recycled plastic blends. Compos Struct 161:469–476
9. Chen J, Teng Z, Wu J (2017) Recycling of waste FRP and corn straw in wood plastic composite. Polym Compos 38(10):2140–2145
10. Nourbakhsh A, Ashori A (2009) Influence of nanoclay and coupling agent on the physical and mechanical properties of polypropylene/bagasse nanocomposite. J Appl Polym Sci 112(3):1386–1390
11. Deka BK, Maji TK, Mandal M (2011) Study on properties of nanocomposites based on HDPE, LDPE, PP, PVC, wood and clay. Polym Bull 67(9):1875–1892
12. Zhang MQ, Rong MZ, Zhang HB, Friedrich K (2003) Mechanical properties of low nano-silica filled high density polyethylene composites. Polym Eng Sci 43(2):490–500
13. Ku H, Wang H, Pattarachaiyakoop N, Trada M (2011) A review on the tensile properties of natural fiber reinforced polymer composites. Compos B Eng 42(4):856–873
14. Mohanty S, Nayak S, Verma S, Tripathy S (2004) Effect of MAPP as a coupling agent on the performance of jute–PP composites. J Reinf Plast Compos 23(6):625–637
15. El-Fattah AA, El Demerdash AGM, Alim Sadik WA, Bedir A (2015) The effect of sugarcane bagasse fiber on the properties of recycled high density polyethylene. J Compos Mater 49(26):3251–3262
16. Zahedi M, Pirayesh H, Khanjanzadeh H, Tabar MM (2013) Organo-modified montmorillonite reinforced walnut shell/polypropylene composites. Mater Des 51:803–809
17. Liu C, Mei C, Xu B, Jiang M, Chen W, Zhou G, Wang K (2019) Effect of the nanosilica content in the shell of coextruded wood-plastic composites to enhance the ultraviolet aging resistance. Polym Adv Technol 30(1):162–169
18. Zahedsheijani R, Faezipour M, Tarmian A, Layeghi M, Yousefi H (2012) The effect of Na+ montmorillonite (NaMMT) nanoclay on thermal properties of medium density fiberboard (MDF). Eur J Wood Wood Prod 70(5):565–571
19. Abd El-Fattah A, Abd ElKader E (2018) Influence of different clays on the mechanical, thermal, and water absorption properties of recycled high-density polyethylene/wood flour hybrid composites. J Compos Mater 52(9):1215–1226
20. Luo X, Benson RS, Kit KM, Dever M (2002) Kudzu fiber-reinforced polypropylene composite. J Appl Polym Sci 85(9):1961–1969
21. Deka BK, Maji TK (2013) Effect of SiO_2 and nanoclay on the properties of wood polymer nanocomposite. Polym Bull 70(2):403–417
22. Awal A, Ghosh S, Sain M (2010) Thermal properties and spectral characterization of wood pulp reinforced bio-composite fibers. J Therm Anal Calorim 99(2):695–701
23. Deka BK, Maji TK (2012) Effect of silica nanopowder on the properties of wood flour/polymer composite. Polym Eng Sci 52(7):1516–1523
24. Khamedi R, Hajikhani M, Ahmaditabar K (2019) Investigation of maleic anhydride effect on wood plastic composites behavior. J Compos Mater 53(14):1955–1962
25. Butylina S, Martikka O, Kärki T (2011) Properties of wood fibre-polypropylene composites: effect of wood fibre source. Appl Compos Mater 18(2):101–111

26. Huang C, Gong M, Chui Y, Chan F (2020) Mechanical behaviour of wood compressed in radial direction-part I. New method of determining the yield stress of wood on the stress-strain curve. J Bioresour Bioprod 5(3):195–204

27. Kord B, Ghalehno MD, Movahedi F (2020) Effect of surface functionalization of SiO_2 nanoparticles on the dynamic mechanical, thermal and fire properties of wheat Straw/LDPE composites. J Polym Environ 28(1):304–316

28. Khakifirouz A, Samariha A, Karbaschi A, Benakachi MA, Beigloo JG (2019) Nanoclay's influence on mechanical and thermal properties of a polypropylene/poplar wood flour nanocomposite. BioResources 14(4):8267–8277

29. Venkatesh G, Deb A, Karmarkar A, Chauhan SS (2012) Effect of nanoclay content and compatibilizer on viscoelastic properties of montmorillonite/polypropylene nanocomposites. Mater Des 37:285–291

30. Hetzer M, De Kee D (2008) Wood/polymer/nanoclay composites, environmentally friendly sustainable technology: a review. Chem Eng Res Des 86(10):1083–1093

31. Faruk O, Matuana LM (2008) Nanoclay reinforced HDPE as a matrix for wood-plastic composites. Compos Sci Technol 68(9):2073–2077

32. Cai X, Riedl B, Zhang S, Wan H (2008) The impact of the nature of nanofillers on the performance of wood polymer nanocomposites. Compos A Appl Sci Manuf 39(5):727–737

33. Rasana N, Jayanarayanan K (2018) Polypropylene/short glass fiber/nanosilica hybrid composites: evaluation of morphology, mechanical, thermal, and transport properties. Polym Bull 75(6):2587–2605

34. Tabari HZ, Nourbakhsh A, Ashori A (2011) Effects of nanoclay and coupling agent on the physico-mechanical, morphological, and thermal properties of wood flour/polypropylene composites. Polym Eng Sci 51(2):272–277

35. Sandquist D, Thumm A, Dickson AR (2020) The influence of fines material on the mechanical performance of wood fiber polypropylene composites. BioResources 15(1):457–468

36. Robledo-Ortíz J, Martín del Campo A, López-Naranjo E, Arellano M, Jasso-Gastinel C, González-Núñez R, Pérez-Fonseca A (2019) Effect of low nanoclay content on the physico-mechanical properties of poly (lactic acid) nanocomposites. Polym Polym Compos 27(2):43–54

37. Hosseini SB, Hedjazi S, Jamalirad L, Sukhtesaraie A (2014) Effect of nano-SiO_2 on physical and mechanical properties of fiber reinforced composites (FRCs). J Indian Acad Wood Sci 11(2):116–121

38. Yadav SM, Yusoh KB (2019) Subsurface mechanical properties and subsurface creep behaviour of modified nanoclay-based wood–plastic composites studied by nanoindentation. Polym Bull 76(5):2179–2196

39. Bazyar B, Samariha A (2017) Thermal, flammability, and morphological properties of nano-composite from fir wood flour and polypropylene. BioResources 12(3):6665–6678

40. Siengchin S (2012) Impact, thermal and mechanical properties of high density polyethylene/flax/SiO_2 composites: effect of flax reinforcing structures. J Reinf Plast Compos 31(14):959–966

41. Rahman MR, Rahman MM, Hamdan S, Lai JCH (2016) impact of maleic anhydride, nanoclay, and silica on jute fiber-reinforced polyethylene biocomposites. BioResources 11(3):5905–5917

42. Mohaiyiddin MS, Ong LH, Akil HM (2013) Preparation and characterization of palm kernel shell/polypropylene biocomposites and their hybrid composites with nanosilica. BioResources 8(2):1539–1550

43. Wan Y, Wu H, Huang L, Zhang J, Tan S, Cai X (2018) Preparation and characterization of corn cob/polypropylene composite reinforced by wood ash. Polym Bull 75(5):2125–2138

44. Onuoha C, Onyemaobi O, Anyakwo C, Onuegbu G (2017) Effect of filler loading and particle size on the mechanical properties of periwinkle shell filled recycled polypropylene composites. Am J Eng Res 6:72–79

45. Sheshmani S, Ashori A, Hamzeh Y (2010) Physical properties of polyethylene–wood fiber–clay nanocomposites. J Appl Polym Sci 118(6):3255–3259

46. Tang Q, Fang L, Guo W (2019) Effects of bamboo fiber length and loading on mechanical, thermal and pulverization properties of phenolic foam composites. J Bioresour Bioprod 4(1):51–59

47. Farsi M (2017) Effect of nano-SiO_2 and bark flour content on the physical and mechanical properties of wood–plastic composites. J Polym Environ 25(2):308–314